

Multilayer-Structured Poly-Vanadium Acid/Polyaniline Composite: Synthesis and Properties for Humidity Sensing

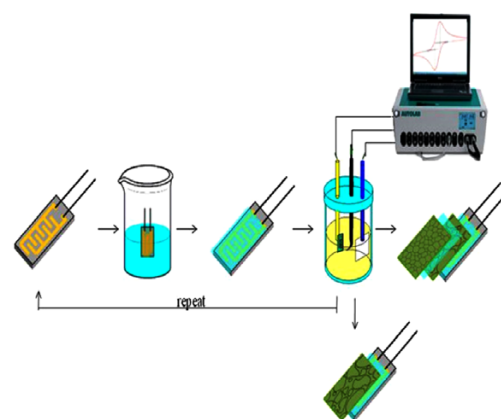
Li Li^{*1}
Yanan Guo¹
Chao Zhao²
Liyuan Song¹

¹Provincial Key Laboratory of Oil & Gas Chemical Technology, College of Chemistry & Chemical Engineering, Northeast Petroleum University, Daqing, 163318, P. R. China

²Oil & Gas field Engineering Department, Jereh Oil & Gas Engineering Corporation, Beijing, 100020, P. R. China

Received August 20, 2017 / Revised December 8, 2017 / Accepted January 25, 2018

Abstract: A high-performance humidity sensor based on multilayer-structured poly-vanadium acid/polyaniline (V/PANI) composite was reported in this paper. Two-layer-structured V/PANI composite was fabricated by dip-coating poly-vanadium acid and electrochemically polymerizing PANI onto the interdigitated gold electrode in sequence, and then the process could be repeated to prepare the second two-layer-structured V/PANI composite. The crystalline phase properties and structural characteristics of the poly-vanadium acid, PANI, and V/PANI composite were characterized by X-ray diffraction (XRD), Fourier transform infrared spectroscopy, and UV-visible spectroscopy, respectively. The morphological characteristics of the first two-layer-structured V/PANI composite and multilayer-structured V/PANI composite were characterized by scanning electron microscopy. Additionally, sensors based on the multilayer-structured V/PANI composite showed good humidity sensing properties. For instance, its impedance changed linearly for approximately four orders of magnitude in a wide range of 11–97% RH. Furthermore, it displayed small hysteresis (~5% RH), fast response ($t_{90\%}$ of 8 s and 12 s for adsorption and desorption processes, respectively), good stability. The possible sensing mechanism was analyzed by considering the special multilayer structure and using complex impedance spectra and the corresponding equivalent circuit of the sensor. The measurement results highlight the multilayer-structured V/PANI composite film is a candidate material for constructing humidity sensors.



Keywords: multilayer-structured, poly-vanadium acid/polyaniline composite, dip-coating, electrochemical synthesis, humidity sensing properties, humidity sensing mechanism.

1. Introduction

In recent years, poly-vanadium acid has been investigated and used as materials for humidity sensors^{1–4} because of its layered structures^{5,6} in which large amounts of foreign cations and water molecules can be intercalated. It shows high sensitivity, short response time and good long-term stability only in low and medium humidity range.^{1,2} The material is not workable in the high humidity range as many absorbed water molecules^{7–9} will destroy the layered structure due to its water solubility. Therefore, it is of importance to improve the long-time stability of poly-vanadium acid in the high humidity range.

There are many research works about sensors built using conducting polymers^{10–13} that have become popular in recent years due to their low cost, ease of synthesis and processing, and ability to sense in room temperature. Of the reported conducting polymers, the polyaniline attracts increasing attention as humidity sensitive materials^{14–17} due to its electrical conductivity and stability. However, PANI-based sensor^{18–20} experiences some disadvantages such as relatively low reproducibility and sensi-

tivity. To overcome these restrictions, PANI is functionalized or frequently used in the form of the composite with different chemical compounds.^{21–28} Lin *et al.*²³ prepared a composite of soluble PANI which was chemically polymerized with a conducting polyelectrolyte and use it as a humidity sensitive material. It is featured with fast response and small hysteresis over almost entire humidity range (0–95% RH), but the recovery time is ~45 s, indicative of quite low sensitivity. Yang *et al.*²⁷ found a bilayer-structured composite humidity sensor based on quaternized and crosslinked poly(4-vinylpyridine) (QC-P4VP) and chemical polymerizing PANI exhibit small hysteresis (about 3% RH), but its response time and recovery time are as long as 24 s and 35 s, respectively. Chen *et al.*²⁸ reported the humidity sensor based on CdS/polyaniline (CdS/PANI) composite with sandwich structure shows excellent humidity properties with a good linearity, fast response-recovery time and good repeatability. Moreover, PANI can be synthesized either chemically or electrochemically. Compared with chemically synthesized PANI, electrochemically synthesized PANI^{29–32} which has no complicated equipment shows better adherence, optical and morphological characteristics and the technique is friendly to the environment.

*Corresponding Author: Li Li (lilytms@nepu.edu.cn)

In this paper, a first two-layer-structured V/PANI composite is fabricated by coating poly-vanadium acid first and electrochemically polymerized polyaniline afterward on the substrate covered with the sensitive film of poly-vanadium acid, then the process could be repeated to prepare the second two-layer-structured V/PANI composite, this is the first ever attempt made to study the multilayer-structured V/PANI composite, which can combine their respective advantages and make up for their deficiency reciprocally as humidity materials. The humidity properties of this material are investigated. The multilayer-structured V/PANI composite exhibit not only fast response and recovery time but also high stability at room temperature. The successful synthesis of multilayer-structured V/PANI composite provides an idea and method for the fabrication of high-performance humidity sensors.

2. Experimental

2.1. Materials

Absolute alcohol and hydrogen peroxide (30 vol%) were obtained from Shenyang East China reagent factory. The aniline monomer, sulphuric acid, and acetone were all obtained from Tianjin Kang Fu Technology Development Co. Ltd. Vanadium pentoxide was supplied by Beijing Chemical Factory. All the reagents were used as received without further purification.

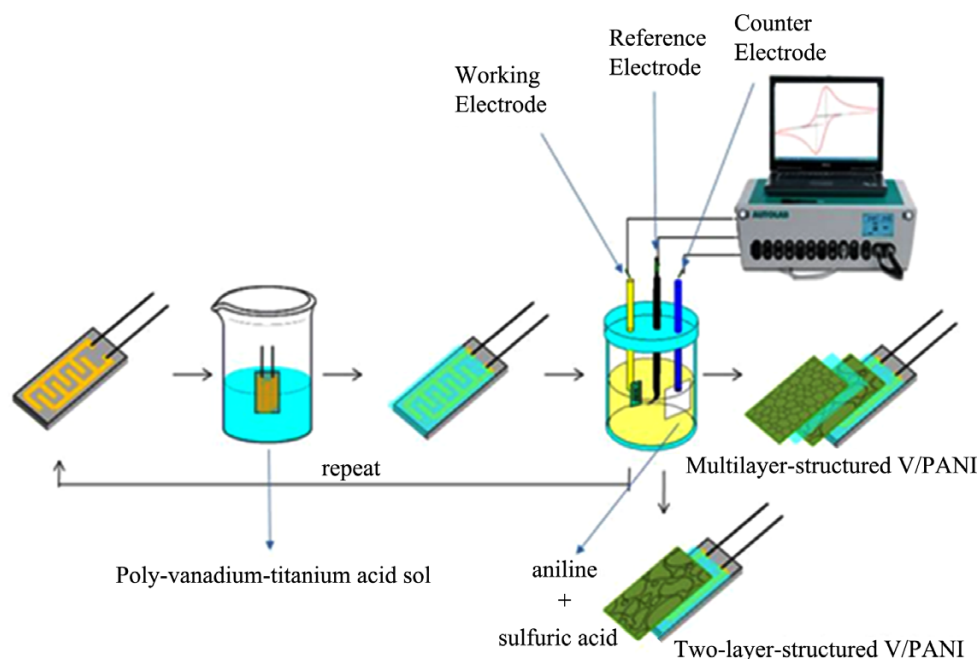
2.2. Synthesis of poly-vanadium acid ($H_2V_{12}O_{31-y} \cdot nH_2O$)

The investigated compounds were produced by the sol-gel technology described in Ref.³³ Typically, 1.3643 g of vanadium pentoxide was dissolved in 25 mL hydrogen peroxide (30%) at 0 °C to obtain a clear solution. Then the solution was heated to 15~20 °C. Keep magnetic stirring until the liquid was almost no particle precipitation, no more produced bubbles, and there

were products sticking to the tube, which indicates the red brown vanadium acid sol was successfully made. Finally, the liquid was cooled down to room temperature in air.

2.3. Preparation of V/PANI composite

A typical preparation process for V/PANI composite was as follows: firstly, the interdigitated gold electrode (IDE) (7 mm×5 mm, 0.7 mm thick) was immersed into the 0.5 mol/L poly-vanadium acid for 30 min. At this time, there was a layer of poly-vanadium acid on the surface of the IDE. Then dry it with nitrogen at the room temperature. The poly-vanadium acid film modified electrode was immersed into the mixed solution of 0.2 mol/L aniline and 0.2 mol/L sulfuric acid, and a layer of polyaniline was electrochemically polymerized by cyclic voltammetry at scan rates of 50 mV/s with sweeping potential between -0.2 and 0.8 V³⁴ for 10 cycles. A three-electrode cell was used, which had the above obtained electrode as working electrode, a platinum net as counter electrode, and Ag/AgCl as reference electrode. After the reaction, the composite film on the IDE can be called a first two-layer-structured V/PANI composite; the process could be repeated to prepare the second two-layer-structured V/PANI composite. Then the working electrode covered with the first two-layer-structured V/PANI composite was immersed in poly-vanadium acid to form a second poly-vanadium acid film, dried and electrochemical polymerized a second layer of polyaniline by cyclic voltammetry. Lastly, the required multilayer-structured V/PANI composite can be obtained. After a certain period, the two-layer-structured V/PANI and multilayer-structured V/PANI composite would be taken out and processed for later use. Schematic view of synthesis of the humidity sensor based on V/PANI composite is shown in Scheme 1. The cyclic voltammetry of the electrochemical polymerization process of the first layer and second layer PANI film was shown in Figure 1 and Figure 2, respectively.



Scheme 1. A schematic diagram of the humidity sensor.

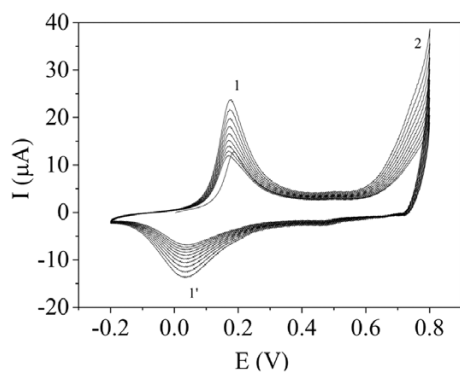


Figure 1. Cyclic voltammometry curves of the first layer PANI film at scan rates of 50 mV/s.

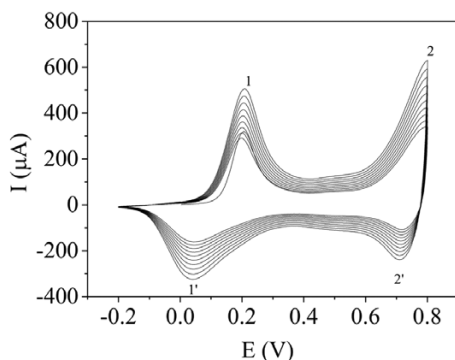


Figure 2. Cyclic voltammometry curves of the second layer PANI film at scan rates of 50 mV/s.

Peak current increases with increasing number of scans which indicates the formation of PANI film. PANI has three oxidation states; (a) the fully reduced leucoemeraldine (LEB), (b) the partially oxidized emeraldine (EM), and (c) the fully oxidized pernigraniline (PNG) state.³⁵ The first set of a redox peak 1-1' in Figure 1 corresponds to the conversion of LEB to EM and the second set of redox couple 2-2' in Figure 2 corresponds to the conversion EM to PNG form.³⁶ Compared to the Figure 1, a significant increase in the current value with applied potential is clearly observed in Figure 2. This is caused mainly because the previously formed layer of polyaniline causes the membrane conductivity better, making the subsequent growth of polyaniline have the access to electrons timely.

2.4. Measurements

The phase identification of the as-prepared multilayer-structured V/PANI composite was carried out by X-ray diffractometer (XRD, Rigaku) using Cu K α radiation ($\lambda=1.5418 \text{ \AA}$) operating at 40 kV and 40 mA. Scanning electron microscopic (SEM) experiments were performed in a SIGMA microscope (Zeiss, Germany). The Fourier transform infrared (FTIR) spectra were recorded on TENSOR 27 Fourier transform infrared spectrometer in the range of 4000 to 500 cm^{-1} . Absorption spectra of the multilayer-structured V/PANI composite were recorded using UV-Vis spectrophotometer (UV-1700, Shanghai). The sensor was successively put into several chambers made of glass which are 18 cm in height and 8 cm in diameter with different RH levels. The characteristic curves of humidity sensitivity were measured on a ZL-5 model LCR analyzer (Shanghai, China) at room temperature ($25 \text{ }^\circ\text{C} \pm 1 \text{ }^\circ\text{C}$). Six different saturated salt solutions LiCl, MgCl_2 , $\text{Mg}(\text{NO}_3)_2$, NaCl, KCl, and K_2SO_4 were used as the humidity generation sources, and the corresponding RH values are 11%, 33%, 54%, 75%, 85%, and 97%, respectively. Complex impedance spectra at different RHs were obtained using a ZL-5 model LCR analyzer (Shanghai, China) over a frequency varying from 12 Hz to 100 kHz with an AC testing voltage of 1 V. The analysis and fitting of the impedance spectra to equivalent circuits were carried out with the ZSIMPWIN software.

3. Results and discussion

3.1. Morphology

The morphology of the samples was characterized by SEM (Figure 3). It can be seen that the two-layer-structured V/PANI humidity sensing element particles are unevenly distributed. Moreover, the multilayer-structured V/PANI sample has uniform shapes.

Figure 3(a) represents small grains of irregular shape. As expected, the Figure 3(b) is all flakes and almost continuous phase morphology. So, the multilayer-structured V/PANI composite film in diagram (b) shows high surface to volume ratio. Moreover, vanadium acid can be covered with the polyaniline particles uniformly. From the two graphs, we could see that (b) is significantly better than (a), mainly because the previously formed

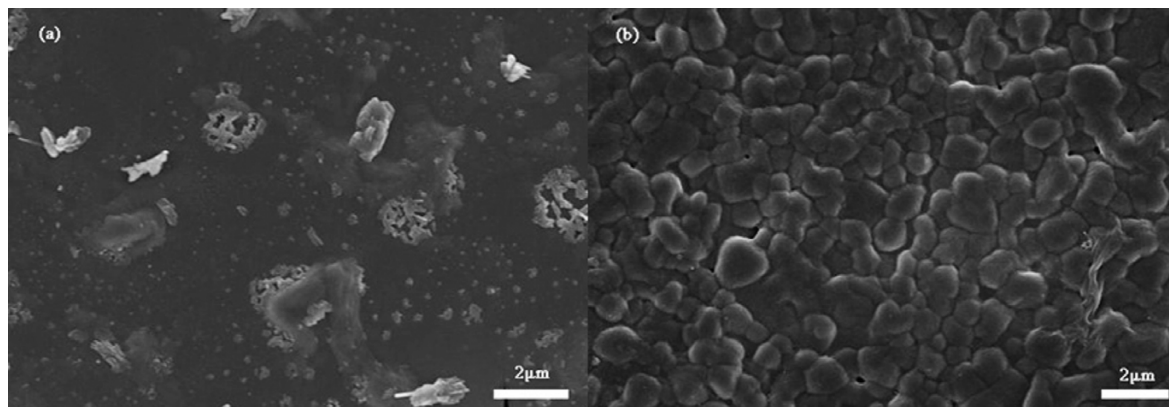


Figure 3. SEM images of (a) two-layer-structured V/PANI and (b) multilayer-structured V/PANI.

layer of polyaniline causes the membrane conductivity better, making the subsequent growth of polyaniline have the access to electrons timely, resulting in the formation of polyaniline more continuous, which corresponding to Figure 1 and Figure 2. So, we choose the multilayer-structured V/PANI composite film as the humidity sensitive material in the following discussion.

3.2. X-Ray diffraction analysis

The structures of poly-vanadium acid, PANI and V/PANI composite were studied by XRD. As shown in Figure 4(a) illustrates the XRD pattern of the $H_2V_{12}O_{31-y} \cdot nH_2O$ which show several diffraction peaks corresponding to (001), (003), (004), and (005). Observed diffraction peaks are in good agreement with previously reported values in the literature.³⁷ Characteristic peak centered at $2\theta=7.840^\circ$ corresponding to the preferential (001) crystallographic direction is clearly observed, and the (001) diffraction peaks are much stronger than (003), (004), and (005). This shows that poly-vanadium acid film is a layered structure having a one-order layered structure which arranges in c-axis. Moreover, the PANI pattern reveals three peaks located at 14.78° , 20.28° , and 25.48° , which are associated with (011), (020), and (200) crystal planes, respectively. The pattern of PANI exhibits peaks at $2\theta=14.78^\circ$ and 25.48° , which were ascribed to the periodicity, perpendicular and parallel to the polymer chain, respectively.³⁸ The (020) reflection at $2\theta=20.28^\circ$ was due to the layers of polymer chains with alternating distance. However, the (001) diffraction peak of poly-vanadium acid disappears in the curve of V/PANI composites, instead, the pattern of poly-vanadium acid displays (004) and (005) diffraction peaks, which are also found in the diffraction patterns of V/PANI composite, revealing the successful preparation the new composites under our conditions. Furthermore, other characteristic peaks of PANI can be found in the pattern of the V/PANI composites. Two broad peaks centered at 20.28° and 25.48° of V/PANI composite are at the same position and more intense than that of pure PANI.³⁹ This result reveals that there are no additional crystalline phases in the V/PANI composite, and poly-vanadium acid which provides surface sites for the deposition of PANI improves the crystallization of it.⁴⁰

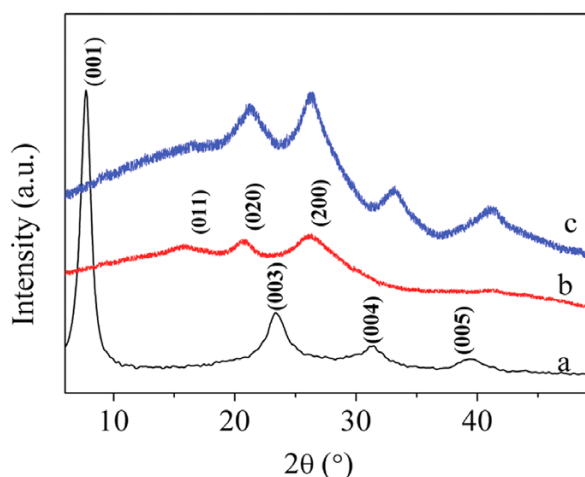


Figure 4. XRD pattern of (a) poly-vanadium acid, (b) pristine PANI, and (c) multilayer-structured V/PANI composite

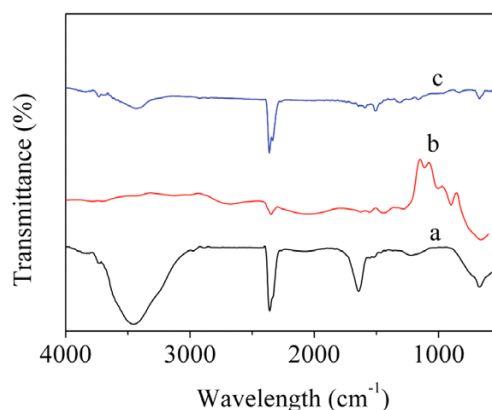


Figure 5. FT-IR spectra of (a) poly-vanadium acid, (b) pristine PANI, and (c) multilayer-structured V/PANI composite.

3.3. IR spectra analysis

FTIR was carried out to study poly-vanadium acid, PANI, and V/PANI composite and shown in Figure 5. The FTIR spectrum of poly-vanadium acid illustrates a broad peak at 3454 cm^{-1} due to the O-H stretching vibration. In addition, the peaks at around 1219 cm^{-1} and 673 cm^{-1} can be attributed to V=O stretching and the V-O-V stretching, respectively. Similarly, the existence of aniline groups is evidenced by the presence of benzene/quinonoid ring vibration at 1500 cm^{-1} and 1650 cm^{-1} .⁴¹ Obviously, the peaks at 1284.53 cm^{-1} , 1118.6 cm^{-1} , and 898.79 cm^{-1} are assigned to C-N stretching vibration, C-N stretching vibration in the benzenoid ring and out-of-plane bending of C-H, respectively.^{42,43} By contrast, these peaks can also be found in the FTIR spectra of V/PANI composite, confirming the successful preparation the new composite.

3.4. UV-visible spectra analysis

UV-vis absorption spectra of PANI and V/PANI composite were obtained in Figure 6. The characteristic peaks at 305 nm, 450 nm and 775 nm of the PANI are due to the $\pi\text{-}\pi^*$ transition, $n\text{-}\pi^*$ transition and π -polaron transition, respectively.^{44,45} In the spectrum of V/PANI composite, the red-shifted band from 305 nm in PANI to 350 nm and the absorption band of PANI at 775 nm moved to 800 nm can be ascribed to the molecule conjugation between PANI and poly-vanadium acid.⁴⁶ The UV-vis spectra with the FT-IR results indicate that PANI and poly-vanadium acid are considered to be combined through electrostatic interactions, hydrogen bonding and $\pi\text{-}\pi$ stacking between the layer components including the positively charged PANI and the negatively charged poly-vanadium acid. This result was also supported by data from the XRD.

3.5. Humidity sensing performance

In order to investigate the best working frequency for the humidity sensor based on V/PANI composite film, the impedance of the sensors was measured as the relative humidity changes from 11% up to 97%, measured at three different frequencies and the results are observed in Figure 7. The impedance difference between

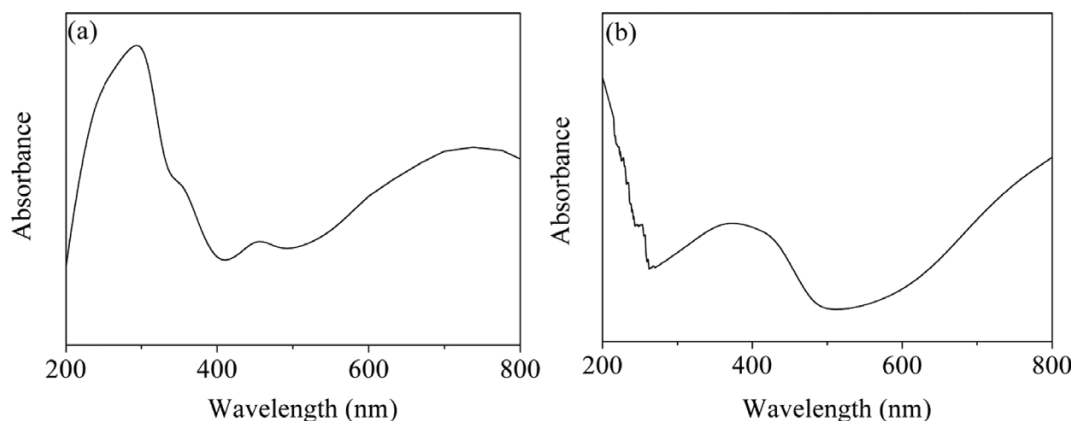


Figure 6. UV-vis spectra of (a) pristine PANI and (b) multilayer-structured V/PANI composite.

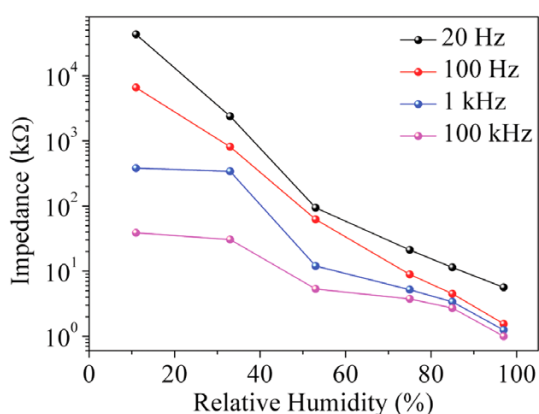


Figure 7. Variations in impedance of the multilayer-structured V/PANI composite based humidity sensor with changes in RH (%) measured at various frequencies measured at 1 V, 25 °C.

adjacent two measuring frequencies becomes progressively smaller with increasing RH⁴⁷ because the polarization of adsorbed water molecules cannot be able to keep pace with the change of electric fields.⁴⁸ Su and Huang⁴⁹ also reported this behavior in the case of carbon nanotubes, where the authors attribute to the effect of high frequency on the adsorption of water molecules. The best linearity of the curve appears at the frequency of 100 Hz. So, 100 Hz can be set as the ideal working frequency of the humidity sensor and used in the following measurements.

The humidity hysteresis characteristic of the multilayer-

structured V/PANI composite sensor is displayed in Figure 8(a). Hysteresis is defined as the maximum humidity difference between the adsorption and desorption curves, which is one of the most important characteristics of a humidity sensor.⁵⁰ The impedance of the sensors was first measured from 11% to 95% RH, and then in the opposite direction. As can be seen, sensor exhibits reversible sensing curves for the humidification and desiccation processes, showing maximum hysteresis of 5% RH, which indicates the good reliability of the sensor. We considered that a uniform distribution of PANI on the surface may be beneficial for a small humidity hysteresis.

The response time and recovery time are important parameters to evaluate the performance of humidity sensor materials. According to literature, the time taken by a sensor to achieve ~90% of total impedance change is defined as the response time and recovery time in case of adsorption and desorption, respectively.⁵¹ It was repeated three times from 11 to 97% RH to prove that the multilayer-structured V/PANI composite sensor humidity sensor showed good impedance repeatability, which could be another advantage. The multilayer-structured V/PANI composite sensor in Figure 8(b) exhibits prompt response and recovery times when the humidity changes, and the response times is 8 s with relative humidity increasing from 11% RH to 97% RH and recovery time is 12 s with relative humidity decreasing from 97% RH to 11% RH. The rapid response and recovery time can be attributed to the high surface to volume ratio of the V/PANI composite which facilitates the transport of water mol-

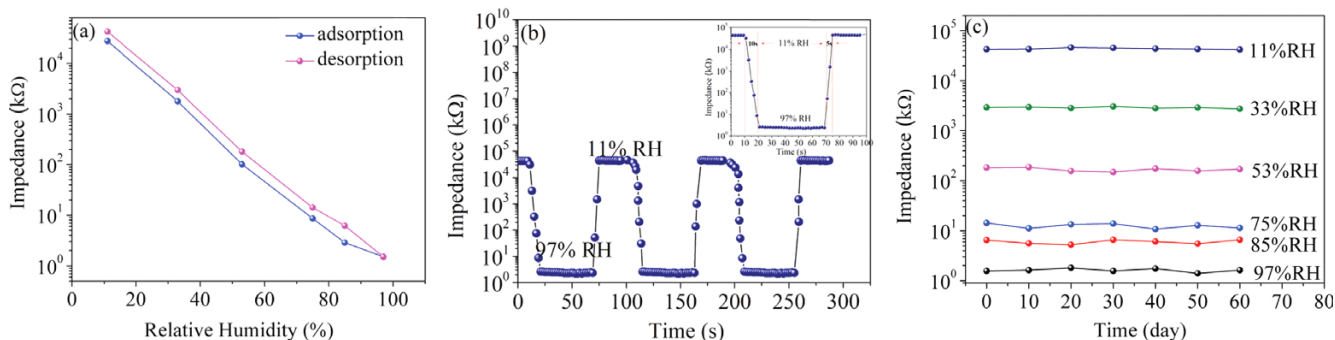


Figure 8. (a) Hysteresis of the multilayer-structured V/PANI composite film with measuring frequency of 100 Hz and AC voltage of 1 V. (b) Response and recovery time of the multilayer-structured V/PANI composite film at 100 Hz. (c) Long-term stability of the multilayer-structured V/PANI composite film.

ecules in the adsorption and desorption processes from the surface of the multilayer-structured V/PANI composite.^{47,48}

Long-term stability is also one of the significant parameters for humidity sensors. The sensor was put in circumstances with RH at 11%, 33%, 54%, 75%, 85%, and 97% for 60 days, respectively, and the impedances were measured every 10 days under various RH. There is an acceptable deviation in the measured impedance in different periods as shown in Figure 8(c), which directly confirms the good long-term stability and reliability of our sensor.

3.6. *I-V* properties of the multilayer-structured V/PANI composite

It is known that, generally, humidity is an important factor that affects humidity sensing performance.⁵² The typical *I-V* characteristics of the V/PANI composite under different relative humidity RH (%) conditions at room temperature are shown in Figure 9. Apparently, at RH (11%, 33%, 54%, 75%, 85%), the studied device exhibits substantial current variations. The good linear behavior of the *I-V* curves clearly indicated the good ohmic behav-

ior of the V/PANI composite. The current of the samples increases remarkably with enhancing RH.⁵³ At 97% RH, measured *I-V* curves showed a nonlinear shape. As could be seen in this figure, the turn-on threshold voltage for this sensor was 4 V. While *I-V* curves had quite a small slope below the applied voltage of 4 V, the current increased rapidly above an applied voltage of 4 V.⁵⁴

At low RH, only a small amount of water molecules can reach the V/PANI composite's surface to form a chemisorption layer, leading to a low conductance. With the increase of humidity levels, the V/PANI composite can effectively absorb water molecules and then serial water layers begin to be formed.⁵⁵ This phenomenon reveals water molecules have an effect on current variation of synthesized composites.

3.7. Discussion on humidity sensitive mechanism

In order to research humidity sensitive mechanism of materials, complex impedance plots of the vanadium-titanium acid/polyaniline composite were measured in the frequency range from 12 Hz to 100 kHz with the RH varied from 11% to 97%. *Z* (re) and *-Z* (im), which stand for the real and imaginary parts of

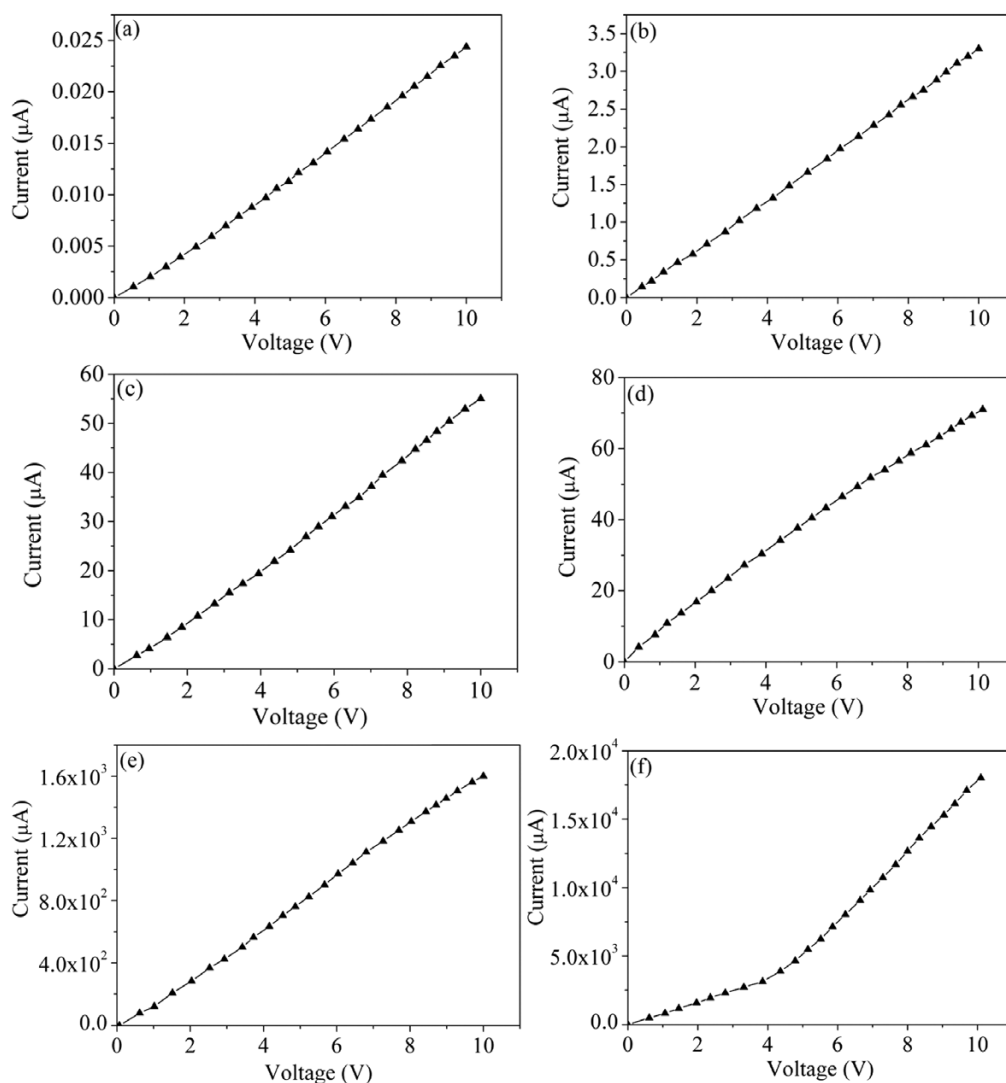


Figure 9. *I-V* curves of the multilayer-structured V/PANI composite under varied RH values at (a) 11%, (b) 33%, (c) 54%, (d) 75%, (e) 85%, and (f) 97% RH.

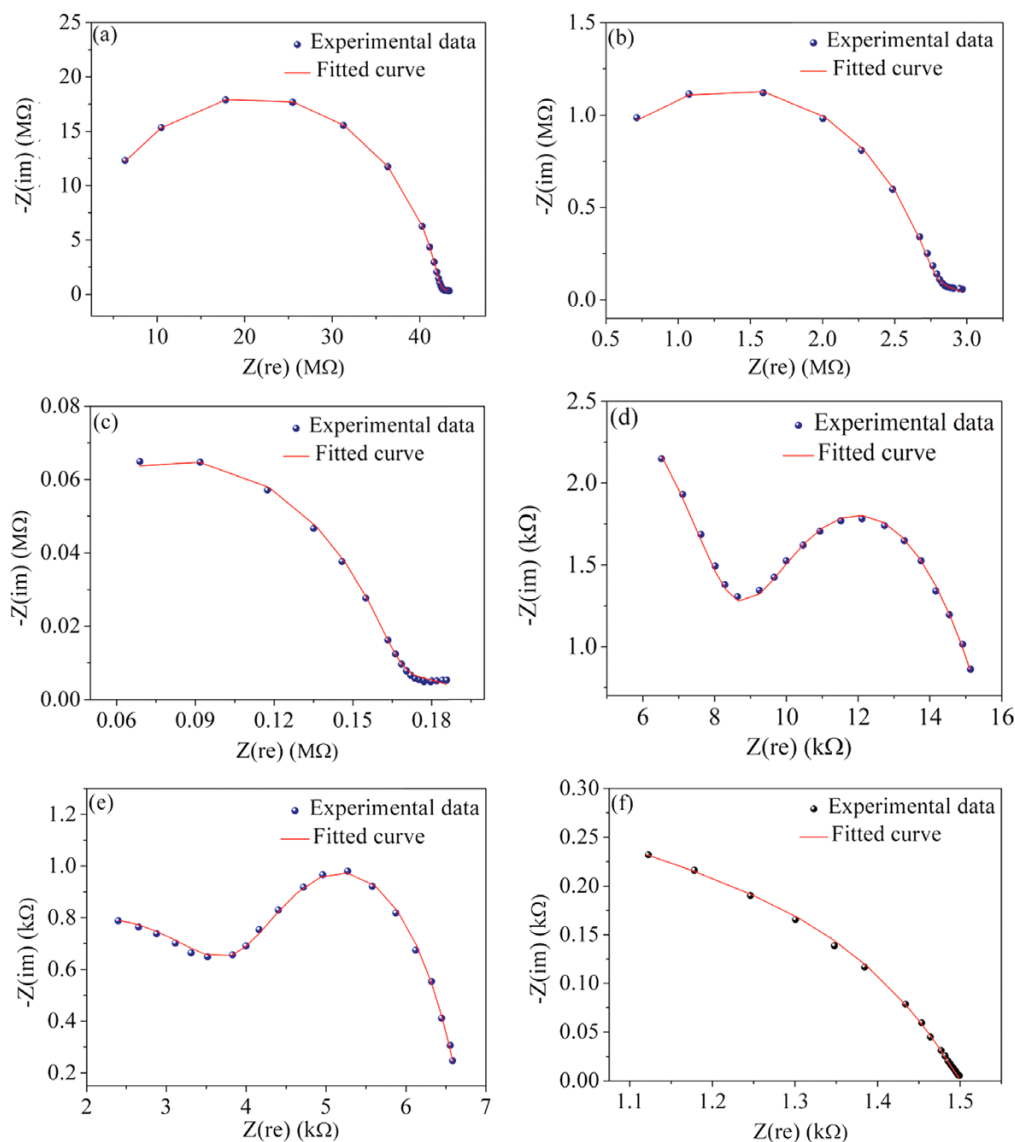


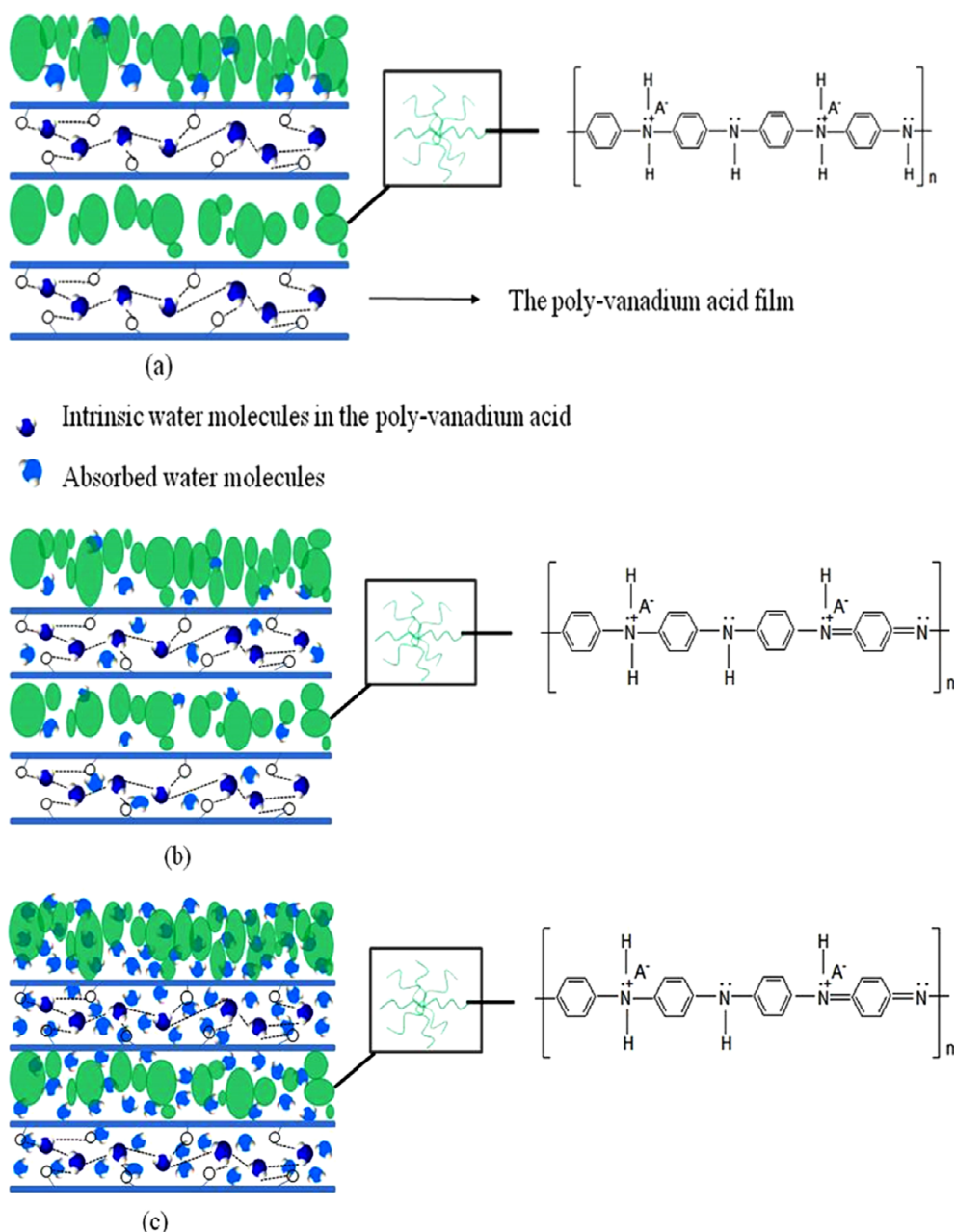
Figure 10. Complex impedance spectra for the multilayer-structured V/PANI composite based humidity sensors recorded at (a) 11%, (b) 33%, (c) 54%, (d) 75%, (e) 85%, and (f) 97% RH.

complex impedance plots, are the horizontal axis and vertical axis, respectively.

In order to understand the sensing mechanism, the typical complex impedance and fitting data curve of the sensor using a ZL-5 model LCR analyzer with the frequency range from 12 Hz to 100 kHz are shown in Figure 10. It is found that the sensing properties of the multilayer-structured V/PANI composite are affected by the special structure and conduction behavior of the poly-vanadium acid and PANI. It can be seen that the complex impedance plots consist of two parts: a semicircle at high frequency and a short straight line at low frequency at RH (11%, 33%, and 54%). The semicircle at high frequency is modeled by an equivalent parallel circuit of the resistance R_1 and capacitance Q_1 of the first two-layer-structured V/PANI film. The short straight line at low frequency is caused by an equivalent parallel circuit of the resistance R_2 and capacitance Q_2 of the second two-layer-structured V/PANI film. When the RH increases to 75% and 85%, pristine semicircle turns into incomplete and small line turns into semicircle gradually. Subsequently,

with the RH increasing to high stage, a small line is observed in high and low-frequency regions. Accordingly, the working principles of the multilayer-structured V/PANI composite and molecular structures of sensing polymer polyaniline are illustrated in Scheme 2.

At RH (11%, 33%, and 54%), depending on the oxidation state of PANI, the PANI structure contains two basic forms: non-oxidized (reduced) and oxidized structures (Scheme 2). The mechanism of reduction is an important phenomenon in conducting polymer film, which is crucial in deciding the increase in the conductivity.⁵⁶ $\text{NH}_2^+ + \text{H}_2\text{O} \rightarrow \text{NH} + \text{H}_3\text{O}^+$. Since in this process a proton is transferred to water by the reaction, absorbed water plays an important role in the conductivity.⁵⁷ So, the H_3O^+ ions hopping across these chemisorbed layers of water molecules is the major source of conduction at low RH.^{58,59} Actually, polyvanadium acid has a contribution to the resistance and capacitance because of its layered structures in which large amounts of water molecules can be intercalated as described in Scheme 2. As with the Table 1, the resistance of the R_1 is found to decrease



Scheme 2. Schematic diagram of the working principle of the multilayer-structured V/PANI composite at (a) RH (11%, 33%, and 54%), (b) RH (75% and 85%), and RH (97%).

as the humidity level increased. On the contrary, the capacitance of the Q_1 is found to increase as the humidity level increased.

The resistance of the R_2 is smaller than R_1 with the RH increase as observed in Table 1, that's may because the second layer PANI is more uniform than the first layer PANI as shown at scanning electron microscopes. In particular, the second two-layer-structured V/PANI composite is more accessible to water than the first two-layer-structured V/PANI composite as described in Scheme 2(a), which makes a contribution to the fact that capacitance of the Q_2 is higher than that of Q_1 .

More and more water molecules are trapped between the poly-vanadium acid and PANI as RH increases (Scheme 2(b)). Consequently, R_1 is much decreased in the environment with humidity levels from RH (54%) to RH (75%). The physisorption

water layers grow with the RH increasing, and finally the internal of the sensing material is fully filled by adsorbed water⁶⁰ at 97% RH as described in Scheme 2(c), so the capacitance also increased sharply. The formation of the conduction path can be explained as the water molecules are mainly adsorbed by physisorption.

Apparently, at low %RH, the bilayer V/PANI composite film not only exhibits low resistance by taking advantage of the high conductivity of the PANI layer, but also demonstrates high capacitance by virtue of the layered structure of the poly-vanadium acid.²⁷ When the RH increased, the water molecules adsorbed by physisorption play a major role in the resistance and capacitance.

Recently, many kinds of materials and methods to prepare

Table 1. Equivalent circuit and corresponding component value under different relative humidities

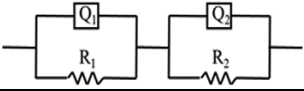
RH		11%	33%	54%	75%	85%	97%
Equivalent							
	Y_{01} (S·s ⁿ /cm ²)	3.669×10^{-13}	5.044×10^{-12}	8.544×10^{-11}	5.578×10^{-9}	5.306×10^{-7}	1.758×10^{-7}
	R_1 (Ω)	4.209×10^7	2.687×10^6	1.588×10^5	8.269×10^3	4.305×10^3	1.301×10^3
Value of element	n_1	0.9053	0.3959	0.3458	0.6825	0.4393	0.5289
	Y_{02} (S·s ⁿ /cm ²)	3.653×10^{-8}	1.742×10^{-7}	2.467×10^{-6}	2.389×10^{-6}	1.523×10^{-6}	6.184×10^{-5}
	R_2 (Ω)	1.623×10^6	3.565×10^5	3.672×10^4	7.834×10^3	2.433×10^3	1.997×10^2
	n_2	0.5084	0.8863	0.8556	0.534	0.7566	0.734

Table 2. Performance of the presented sensor in this work compared with previous work

Sensing material	Fabrication method	Hysteresis	Response/Recovery time	Stability	Ref.
PANI/PSSA/PVA	dip coating	~2% RH	6 s/10 s	not good	61
PANI-PSSA/PEO/PVB	in-situ	~1% RH	8 s/6 s	good	62
QC-P4VP/PANI	deposition	~3% RH	24 s/35 s	good	27
CdS/PANI	in-situ	~0.5% RH	not mentioned	good	28
PANI	electrospinning	~1% RH	8 s/6 s	not mentioned	24
PANI/IPN-PE	deposition	~1% RH	7 s/7 s	not mentioned	23
LiAl-LDH/PANI/SDS	dip coating	~5.2% RH	30 s/2 s	good	18
MgAl-LDH/PANI/SDS	dip coating	~4.5% RH	3 s/25 s	good	18
NiAl-LDH/PANI/SDS	dip coating	~3.2% RH	4 s/25 s	good	18
V/PANI	electrochemical synthesis	~5% RH	8 s/12 s	good	This work

humidity sensors have been investigated. Table 2 shows the performance comparison between our work with those reported modified electrodes with PANI humidity sensors in previous works,^{18,23,24,27,28,61,62} in terms of the sensor material, fabrication method, hysteresis, response/recovery time and sensitivity. We can find that the multilayer-structured poly-vanadium acid/polyaniline composite could offer a great potential for applications.

4. Conclusions

Multilayer-structured V/PANI composite was successfully synthesized. In addition, the XRD, UV-vis spectra and the FTIR results were studied in detail to investigate the polymerization mechanism for the formation of V/PANI composite. The good humidity sensing characteristics of the composite sensor might relate to the special multilayer-structured configuration. Both PANI and the poly-vanadium acid play an important role in realizing good humidity sensing properties of the composite. These results illustrate that the fast response to the humidity could be attributed to the PANI that completely cover the surface. Additionally, the mechanism of humidity sensors based on the multilayer-structured V/PANI composite was investigated in details. The multilayer-structured V/PANI composite not only exhibits low resistance by taking advantage of the high conductivity of the PANI layer, but also demonstrates high capacitance by virtue of the layered structure of the poly-vanadium acid. When the RH increased, the water molecules adsorbed by physisorption play a major role in the resistance and capacitance. The composite is promising as a new humidity sensitive material for measuring humidity.

References

- (1) J. Bullet, P. Cordier, O. Gallais, M. Gauthier, and F. Babonneau, *J. Non-Cryst. Solids*, **68**, 135 (1984).
- (2) P. Barboux, N. Baffier, R. Morineau, and J. Livage, *Solid State Ionics*, **9**, 1073 (1983).
- (3) J. E. Moneyron, A. de Roy, and J. P. Besse, *Sens. Actuators B: Chem.*, **4**, 189 (1991).
- (4) V. Bondarenka, S. Grebinskij, S. Mickevičius, V. Volkov, and G. Zacharova, *Sens. Actuators B: Chem.*, **28**, 227 (1995).
- (5) G. S. Zakharova, V. L. Volkov, M. A. Uimin, A. A. Mysik, and A. E. Ermakov, *Inorg. Mater.*, **46**, 1115 (2010).
- (6) B. Casal, E. Ruizhitzky, M. Crespin, D. Tinet, and J. C. Galván, *J. Chem. Soc. Faraday Trans. 1*, **85**, 4167 (1989).
- (7) I. A. Leonidov, V. L. Volkov, G. S. Zakharova, and O. N. Leonidova, *Inorg. Mater.*, **38**, 1178 (2002).
- (8) V. Bondarenka, S. Grebinskij, S. Mickevičius, H. Tvardauskas, Z. Martūnas, V. Volkov, and G. Zakharova, *Sens. Actuator, B Chem.*, **55**, 60 (1999).
- (9) S. Mickevičius, V. Bondarenka, S. Grebinskij, V. Volkov, and G. Zakharova, *The Workshop on Sesens*, 2000.
- (10) M. V. Kulkarni, S. K. Apte, S. D. Naik, J. D. Ambekar, and B. B. Kale, *Sens. Actuators B: Chem.*, **178**, 140 (2013).
- (11) W. P. Chen, Z. G. Zhao, X. W. Liu, Z. X. Zhang, and C. G. Suo, *Sensors*, **9**, 7431 (2009).
- (12) Z. Zhu, T. Horiuchi, K. Kruusamäe, L. Chang, and K. Asaka, *J. Phys. Chem. B*, **120**, 3215 (2016).
- (13) P. Li, Y. Li, B. Ying, and M. Yang, *Sens. Actuator, B Chem.*, **141**, 390 (2009).
- (14) D. Nicolas-Debarnot and F. Poncin-Epaillard, *Anal. Chim. Acta*, **475**, 1 (2003).
- (15) S. T. McGovern, G. M. Spinks, and G. G. Wallace, *Sens. Actuators B: Chem.*, **107**, 657 (2005).
- (16) R. Nohria, R. K. Khillan, Y. Su, R. Dikshit, Y. Lvov, and K. Varahramyan, *Sens. Actuator B: Chem.*, **114**, 218 (2006).

- (17) A. T. Ramaprasad and V. Rao, *Sens. Actuator B: Chem.*, **148**, 117 (2010).
- (18) X. Z. Li, S. R. Liu, and Y. Guo, *RSC Adv.*, **6**, 63099 (2016).
- (19) F. W. Zeng, X. X. Liu, D. Diamond, and K. T. Lau, *Sens. Actuator B: Chem.*, **143**, 530 (2010).
- (20) S. K. Shukla, A. Bharadvaja, A. Tiwari, G. K. Parashar, and G. C. Dubey, *Adv. Mater. Lett.*, **1**, 129 (2010).
- (21) A. A. Athawale and M. V. Kulkarni, *Sens. Actuators B: Chem.*, **67**, 173 (2000).
- (22) M. L. Singla, S. Awasthi, and A. Srivastava, *Sens. Actuators B: Chem.*, **127**, 580 (2007).
- (23) L. Peng, L. Yang, L. Hong, Y. Chen, and M. Yang, *Mater. Chem. Phys.*, **115**, 395 (2009).
- (24) Q. Lin, Y. Li, and M. Yang, *Anal. Chim. Acta*, **748**, 73 (2012).
- (25) K. C. Sajjan, A. S. Roy, A. Parveen, and S. Khasim, *J. Mater. Sci. Mater. Electron.*, **25**, 1237 (2014).
- (26) N. Wang, J. Li, W. Lv, J. Feng, and W. Yan, *RSC Adv.*, **5**, 21132 (2015).
- (27) Y. Li, K. Fan, H. Ban, and M. Yang, *Synth. Met.*, **199**, 51 (2015).
- (28) Q. Q. Chen, M. X. Nie, and Y. Guo, *Sens. Actuators B: Chem.*, **254**, 30 (2018).
- (29) S. J. Choi and S. M. Park, *J. Electrochem. Soc.*, **149**, 26 (2002).
- (30) N. Parvatikar, S. Jain, S. Khasim, M. Revansiddappa, S. V. Bhoraskar, and M. V. N. A. Prasad, *Sens. Actuator, B Chem.*, **114**, 599 (2006).
- (31) N. Parvatikar, S. Jain, S. V. Bhoraskar, and M. V. N. A. Prasad, *J. Appl. Polym. Sci.*, **102**, 5533 (2010).
- (32) N. Parvatikar, S. Jain, C. M. Kanamadi, B. K. Chougule, S. V. Bhoraskar, and M. V. N. A. Prasad, *J. Appl. Polym. Sci.*, **103**, 653 (2010).
- (33) V. L. Volkov, G. S. Zakharova, V. G. Zubkov, and A. A. Ivakin, *J. Neorg. Chem. (in Russian)*, **31**, 642 (1985).
- (34) C. Q. Cui, L. H. Oing, T. C. Tan, and J. Y. Lee, *Electrochim. Acta*, **38**, 1395 (1993).
- (35) R. Sha, K. Komori, and S. Badhulika, *Electrochim. Acta*, **233**, 44 (2017).
- (36) E. Song and J. W. Choi, *Nanomaterials*, **3**, 498 (2013).
- (37) K. Pragna, G. Hyettb, and R. Binionsa, *Adv. Mater. Lett.*, **1**, 86 (2010).
- (38) K. R. Reddy, K. P. Lee, and A. I. Gopalan, *J. Appl. Polym. Sci.*, **106**, 1181 (2007).
- (39) K. R. Reddy, K. P. Lee, and A. I. Gopalan, *Colloids Surf. A*, **320**, 49 (2008).
- (40) K. R. Reddy, M. J. Han, Y. Lee, and A. V. Raghu, *J. Polym. Sci., Part A: Polym. Chem.*, **48**, 1477 (2010).
- (41) Y. P. Zhang, S. H. Lee, K. R. Reddy, A. I. Gopalan, and K. P. Lee, *J. Appl. Polym. Sci.*, **104**, 2743 (2007).
- (42) K. R. Reddy, K. V. Karthik, S. B. B. Prasad, S. K. Soni, M. J. Han, and A. V. Raghu, *Polyhedron*, **120**, 169 (2016).
- (43) K. R. Reddy, K. P. Lee, A. I. Gopalan, and A. M. Showkat, *Polym. J.*, **38**, 349 (2006).
- (44) K. R. Reddy, B. C. Sin, K. S. Ryu, J. C. Kim, H. Chung, and Y. Lee, *Synth. Met.*, **159**, 595 (2009).
- (45) K. R. Reddy, K. P. Lee, and A. I. Gopalan, *J. Nanosci. Nanotechnol.*, **7**, 3117 (2007).
- (46) K. R. Reddy, K. P. Lee, Y. Lee, and A. I. Gopalan, *Mater. Lett.*, **62**, 1815 (2008).
- (47) V. R. Khadse, S. Thakur, K. R. Patil, P. Patil, V. R. Khadse, and S. Thakur, *Sens. Actuators B: Chem.*, **203**, 229 (2014).
- (48) J. Zhang, L. Sun, C. Chen, M. Liu, W. Dong, and W. Guo, *J. Alloys Compd.*, **695**, 520 (2017).
- (49) M. Alifanti, B. Baps, N. Blangenois, J. Naud, P. Grange, and B. Delmon, *Chem. Mater.*, **15**, 395 (2003).
- (50) V. K. Tomer, P. V. Adhyapak, S. Duhan, and I. S. Mulla, *Micropor. Mesopor. Mater.*, **197**, 140 (2014).
- (51) V. K. Tomer, S. Duhan, P. V. Adhyapak, and I. S. Mulla, *J. Am. Ceram. Soc.*, **98**, 741 (2015).
- (52) H. I. Chen, K. C. Chuang, C. H. Chang, W. C. Chen, I. P. Liu, and W. C. Liu, *Sens. Actuators B: Chem.*, **246**, 408 (2017).
- (53) C. L. Hsu, L. F. Chang, and T. J. Hsueh, *Sens. Actuators B: Chem.*, **249**, 265 (2017).
- (54) W. Li, M. Hu, P. Ge, J. Wang, and Y. Y. Guo, *Appl. Surf. Sci.*, **317**, 970 (2014).
- (55) L. Wang, Y. He, J. Hu, Q. Qi, and T. Zhang, *Sens. Actuators B: Chem.*, **153**, 460 (2011).
- (56) S. Jain, S. Chakane, A. B. Samui, V. N. Krishnamurthy, and S. V. Bhoraskar, *Sens. Actuators B: Chem.*, **96**, 124 (2003).
- (57) P. Park, Application of nano-structured conducting polymers to humidity sensing, *Dissertations & Theses - Gradworks*, 2008.
- (58) V. K. Tomer and S. Duhan, *Sens. Actuators B: Chem.*, **212**, 517 (2015).
- (59) R. Wang, T. Zhang, Y. He, X. Li, W. Geng, J. Tu, and Q. Yuan, *J. Appl. Polym. Sci.*, **115**, 3474 (2010).
- (60) H. Zhao, T. Zhang, J. Dai, K. Jiang, and T. Fei, *Sens. Actuators B: Chem.*, **240**, 681 (2017).
- (61) Y. Li, B. Ying, L. Hong, and M. Yang, *Synth. Met.*, **160**, 455 (2010).
- (62) Q. Lin, Y. Li, and M. Yang, *Sens. Actuators B: Chem.*, **161**, 967 (2012).